

Multicast Scheduling over Multiple Channels: A Distribution-Embedding Deep Reinforcement Learning Method

Ran Li, Chuan Huang, Xiaoqi Qin, and Shengpei Jiang

Abstract

Multicasting is an efficient technique to simultaneously transmit common messages from the base station (BS) to multiple mobile users (MUs). The multicast scheduling problem over multiple channels, which jointly minimizes the energy consumption of the BS and the latency of serving asynchronized requests from the MUs, is formulated as an infinite-horizon Markov decision process (MDP) with large discrete action space, multiple time-varying constraints, and multiple time-invariant constraints, which has not been efficiently solved in the literatures. To address this problem, this paper proposes a novel algorithm called distribution-embedding multi-agent proximal policy optimization (DE-MAPPO), which consists of two parts: a modified MAPPO module and a distribution-embedding module. The former one modifies MAPPO's offline training and online applying mechanisms to handle the large discrete action space issue and time-varying constraints, and the latter one iteratively adjusts the action distribution to satisfy the time-invariant constraints. Moreover, as a benchmark, a performance upper bound of the considered MDP is derived by solving a two-step optimization problem. Numerical experiments show that the proposed algorithm achieves comparable performance to the derived benchmark in typical scenarios.

Index Terms

This work was presented in part at the 2022 IEEE/CIC International Conference on Communications in China [1].
(Corresponding author: Chuan Huang.)

R. Li and C. Huang are with the School of Science and Engineering (SSE) and the Future Network of Intelligence Institute (FNii), The Chinese University of Hong Kong, Shenzhen 518172, China, (e-mails: ranli2@link.cuhk.edu.cn; huangchuan@cuhk.edu.cn).

X. Qin is with the State Key Laboratory of Networking and Switching Technology, Beijing University of Posts and Telecommunications, Beijing 100876, China, (e-mail: xiaoqin@bupt.edu.cn).

S. Jiang is with the SF Technology, Shenzhen 518052, China, (e-mail: philip.jiang@sffmail.sf-express.com).

Multicast, large discrete action space, time-varying constraints, time-invariant constraints, distribution-embedding multi-agent proximal policy optimization (DE-MAPPO)

I. INTRODUCTION

The number of mobile users (MUs) and mobile data traffic keep increasing rapidly in recent years. In 2023, the number of smartphones has reached 6.65 billion, meaning that 82.92% of the world's population owns a smartphone [2]. Meanwhile, mobile data traffic has reached 108 exabytes per month, which is 4-fold of the monthly data traffic in 2018 [3]. Remarkably, video data traffic, including live streaming, virtual reality (VR) video, and augmented reality (AR) video, which has a high similarity among the contents requested by different MUs, makes up more than 70 percentage of the total mobile data traffic in 2023 [3]. The current cellular systems can hardly fulfill such heavy tasks with the unicast technique for the downlink transmissions, by which the base station (BS) assigns individual channel to each MU's request. By exploiting the similarity of the data requests, multicast technique can temporarily hold the MU's requests until there are sufficient amount of them, and then serve them simultaneously during one multicast transmission. Apparently, exploiting multicast in the future cellular network could significantly improve the energy efficiency (defined as the average energy cost per request) [4]. Notably, the asynchronous requests from multiple MUs would be served with different latencies in this multicast mechanism. Therefore, it is of great interest to balance the energy efficiency and the average latency of the considered multicast scheme in the cellular networks.

A. Related works

In recent years, many works have studied the multicast scheduling problem in the cellular networks, especially in the 5G era where the cellular networks are assisted by the advanced techniques such as millimeter wave (mmWave) communication [5], non-orthogonal multiple access (NOMA) [6], and intelligent reflecting surface (IRS) [7]. One major goal is to maximize the system throughput with limited resources, and approaches including deep reinforcement learning (DRL), beamforming, were validated to have promising performances in [5], [7]–[9]. Along another research avenue, due to the increasing public attention to green communications, energy efficiency maximization becomes more compelling in the recent researches [6], [10]–[12] and aims to serve more requests with as little energy as possible. To tackle this issue, the authors in [6], [10] utilized beamforming and designed the optimal precoders at the BS to maximize

the energy efficiency for the NOMA and mmWave systems, respectively. The authors in [11] discussed the device-to-device assisted multicast scheduling problems for the mmWave system, and proposed a supervised learning method to maximize the energy efficiency. The authors in [12] discussed the joint unicast-multicast scheduling for the NOMA system, and proposed a rate-splitting method to optimize both the spectral and energy efficiency. Another major concern for multicast scheduling is the fairness issue, which aims to balance the latencies among different MUs [13], [14]. Obviously, the methods only optimizing the energy efficiency in [6], [10]–[12] prefer to allocate resources to the MUs with better channel condition, whereas the MUs with poor channel condition would be served with more latencies and may even be abandoned by the BS. To jointly optimize the energy efficiency and the fairness, namely the proportional fairness [15], a wise choice is to optimize the summation of the logarithm transmission rates of all MUs [16], where, due to the “strictly concave” and the “increasing” features of the logarithm function, improving the already high transmission rate for the good-channel-condition MUs is inferior to serving the MUs with poor channel condition. Another approach is to gather the MU’s requests into request queues [17]. By utilizing the Lyapunov optimization, the rate stability of the request queues was established, which ensures finite latencies for the MUs’ requests. However, the proposed algorithms in [16], [17] only gave a rough control on the latency to be finite, and the precise dominations, such as minimizing the latency subject to certain constraints, are difficult under these frameworks.

To jointly optimize the energy efficiency and the latency in a more flexible way, the most common approach is to minimize the weighted summation of them [18]–[21]. However, since the information about the accumulated requests from the MUs is required to compute the latency, the multicast scheduling problem was formulated as an infinite-horizon Markov decision process (MDP), which is a commonly known difficult problem due to “the curse of dimensionality” [22]. The authors in [18]–[21] proposed some low-complexity methods to solve this problem. Specifically, the authors in [18] studied the multicast scheduling problem where multiple MUs request one common message and the MUs have mixed latency penalties, and a suboptimal scheduling policy was developed based on the optimal stopping theorem. The authors in [19] discussed the multicast scheduling problem with multiple requested messages and single available channel, and the optimal scheduling policy was constructed based on the classical relative value iteration (RVI) algorithm. The authors in [20], [21] deployed DRL algorithms to study the joint multicast scheduling and message caching problems in the ultra dense networks and the

heterogeneous networks, respectively, and again focused on the scenarios with multiple requested messages and single available channel. Notably, the authors in [18]–[21] assumed that the multicasting of each message on each channel starts and ends synchronously, i.e., all channels are always released from multicastings simultaneously and available at every scheduling moment.

To the best of our knowledge, there is no existing work discussed the scheduling problem for asynchronous multicasting, where the multicastings of different messages over different channels consume different time durations and thus different multicastings would start and end in an asynchronous manner.

B. Main contributions

This paper studies a general multicast scheduling problem in the cellular networks: a) multiple MUs randomly request multiple messages, which are stored at the BS in advance with the cache technique [20], [21]; b) multiple channels are available for multicast transmissions at the BS; c) the multicasting of different sizes of messages over different channels consumes different time durations, i.e., asynchronous multicasting. d) the optimal multicast scheduling policy is supposed to strike the optimal tradeoff between the energy efficiency and the latency penalty. We summarize our contributions as follows:

- We formulate the multicast scheduling problem as an infinite-horizon MDP, which is challenging due to the large discrete action space, multiple time-varying constraints, and multiple time-invariant constraints. To address these challenges, we convert this problem into an equivalent Markov game and propose the distribution-embedding multi-agent proximal policy optimization (DE-MAPPO) to efficiently solve it, which consists of a modified MAPPO and a distribution-embedding module. The modified MAPPO adopts the structure proposed in [23] and is capable to address the large discrete action space issue and time-varying constraints. The proposed distribution-embedding module modifies the output distribution of MAPPO iteratively to address the time-invariant issue and achieves better convergence performance than the conventional action-embedding approach.
- We derive a performance upper bound for the considered MDP, which works as the performance benchmark to evaluate the proposed DE-MAPPO. First, we prove that the time-varying constraints in the MDP problem can be simplified as a set of time-invariant constraints, which reveal the statistical features of the policies satisfying the time-varying constraints. Then, we convert the simplified problem into a two-step optimization problem:

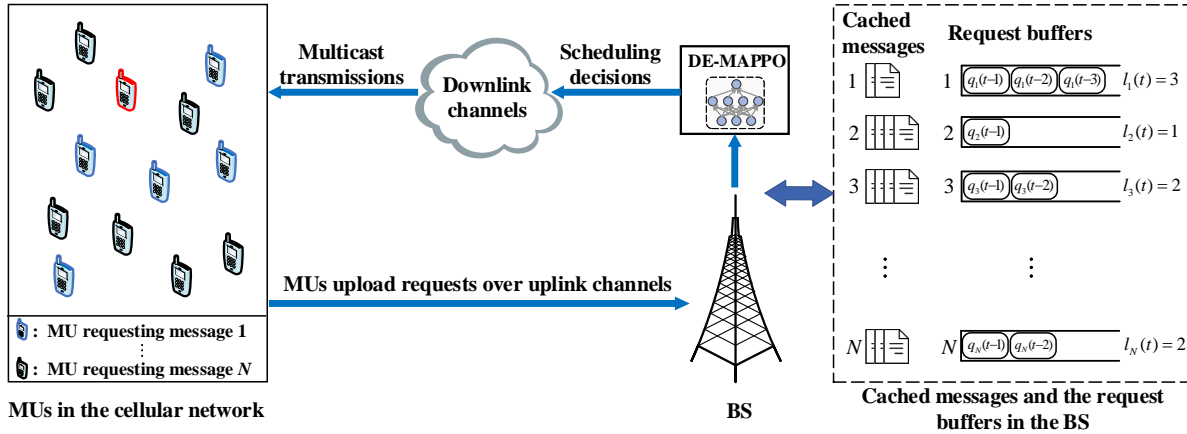


Figure 1: Multicast schedule over multiple channels.

The first step minimizes the latency penalty and is decomposed into multiple independent subproblems, which can be formulated as simple MDPs and can be solved by vanilla deep Q network (DQN) or optimal stopping rule; the second step jointly minimizes the energy consumption and the latency penalty and is formulated as a naive constrained maximization problem, which is solved by integer programming or Lagrange multiplier technique. Solving the optimizations of the two steps gives the performance benchmark.

The remainder of this paper is organized as follows. Section II introduces the system model and formulates the multicast scheduling problem. Section III presents the proposed algorithm. Section IV discusses the upper bound benchmark of the multicast networks. Section V evaluates the performance of the proposed algorithm. Finally, Section VI concludes this paper.

II. SYSTEM MODEL AND PROBLEM FORMULATION

Consider a slotted cellular network as depicted in Fig. 1, which includes a single base station (BS) that caches N messages and a large number of mobile users (MUs). During each time slot, MUs can upload requests for downloading one or more of the cached messages from the BS. At the end of each time slot (or at the beginning of the next time slot), the BS catalogs all the requests from the MUs and stores the number of new requests for each of the N messages in N request buffers. Instead of immediately multicasting the message requested by the buffered requests, the BS may choose to delay the multicast transmission for several time slots. By doing so, the BS can accumulate more requests for each message and serve a larger number of MUs simultaneously in a single transmission, thereby conserving transmission energy. We assume that

there are M downlink channels available for multicast transmissions, and that the multicasting of N messages may last for multiple consecutive time slots, depending on their sizes. In the following, we formulate the multicast scheduling problem for the above multi-message and multi-channel system as an infinite-horizon Markov decision process (MDP).

1) *State*: The state contains *request matrix*, *channel availability*, and *channel status*.

Request matrix: Denote the number of the requests for the n^{th} message arriving within the t^{th} time slot as $q_n(t)$, which follows Poisson distribution as $q_n(t) \sim \text{Pois}(\lambda_n)$, and the number of time slots after the previous multicasting of the n^{th} message as $l_n(t) \in \mathbb{N}$, where \mathbb{N} is the set of 0 and all natural numbers. Then, within the past $l_n(t)$ time slots, all the arrived requests for the n^{th} message are stored in the n^{th} request buffer of the BS, and we represent these requests by the *request vector* $\mathbf{q}_n(t)$, which is defined as

$$\mathbf{q}_n(t) \triangleq \begin{cases} \left[\begin{array}{c} q_n(t-1), \dots, q_n(t-l_n(t)), \\ \underbrace{0, \dots, 0}_{M^*-l_n(t) \text{ zeros}} \end{array} \right]^T & l_n(t) \leq M^* \\ \left[\begin{array}{c} q_n(t-1), \dots, q_n(t-M^*+1), \\ \sum_{\tau=M^*}^{l_n(t)} q_n(t-\tau) \end{array} \right]^T & l_n(t) > M^*. \end{cases} \quad (1)$$

Here, M^* is the size of the request buffer and if $l_n(t) > M^*$, the requests arriving before the $(t-M^*)^{\text{th}}$ time slot are accumulated in the last entry of $\mathbf{q}_n(t)$. Finally, define the *request matrix* as $\mathbf{Q}(t) \triangleq [\mathbf{q}_1(t), \mathbf{q}_2(t), \dots, \mathbf{q}_N(t)]^T$, which has the dimensionality of N -by- M^* .

Channel availability: We consider each multicast transmission of the n^{th} message over the m^{th} channel to consume $T_{n,m} \in \mathbb{Z}^+$ consecutive time slots, where \mathbb{Z}^+ denotes the set of all positive integers. During these time slots, the m^{th} channel is not available for new multicasting. To keep track of the availability of the m^{th} channel, we define $c_m(t)$ as the availability of the m^{th} channel at the t^{th} time slot: If the m^{th} channel is neither scheduled nor reserved for a previous multicast transmission, $c_m(t)$ is set to 0; otherwise, $c_m(t)$ is the number of remaining time slots before the m^{th} channel is released. Finally, we represent the availability of all channels at the t^{th} time slot as a vector $\mathbf{c}(t) = [c_1(t), c_2(t), \dots, c_M(t)]^T$, which we refer to as the *channel availability vector*.

Channel status: The downlink channel gain from the BS to the q^{th} MU that has requested the n^{th} message within the t^{th} time slot over the m^{th} channel is denoted as $g_{n,m,q}(t)$. This channel gain is assumed to follow slow fading and be constant until the q^{th} MU is served. It is worth

noting that the overall performance of the multicast transmission is determined by the worst downlink channel gain among the MUs. To be more precise, at the beginning of the t^{th} time slot, we only need to consider the MU with the worst channel gain among those whose requests are buffered in $\mathbf{q}_n(t)$, which can be expressed as:

$$g_{n,m}(t) \triangleq \min_{\tau \in \{1, \dots, l_n(t)\}} \left\{ \min_{q \in \{1, \dots, q_n(t-\tau)\}} \{g_{n,m,q}(t-\tau)\} \right\}. \quad (2)$$

Finally, we denote the *channel status* as a N -by- M -dimension matrix $\mathbf{G}(t)$, with the $(n, m)^{\text{th}}$ entry of $\mathbf{G}(t)$ being $g_{n,m}(t)$, i.e., $[\mathbf{G}(t)]_{(n,m)} \triangleq g_{n,m}(t)$.

To summary, the state of the considered system at the t^{th} time slot is the triple $\mathbf{s}(t) \triangleq (\mathbf{Q}(t), \mathbf{c}(t), \mathbf{G}(t))$ and thus the state space has the dimensionality of $NM^* + M + NM$.

2) *Action*: Denote the multicast scheduling decision for the m^{th} channel in the beginning of the t^{th} time slot as $a_m(t) \in \{0, 1, \dots, N\}$. Specifically, $a_m(t) > 0$ means to multicast the $a_m(t)^{\text{th}}$ message over the m^{th} channel in the beginning of the t^{th} time slot; $a_m(t) = 0$ means that the m^{th} channel is not scheduled to multicast any message. Denote the multicast scheduling decision for all channels as $\mathbf{a}(t)$, i.e., $\mathbf{a}(t) \triangleq [a_1(t), a_2(t), \dots, a_M(t)]^T$, and obviously, $\mathbf{a}(t)$ is the action of the considered system. Notably, if the m^{th} channel has been reserved for multicasting in previous slots, i.e., $c_m(t) > 0$, it cannot be scheduled to multicast any new message. That is,

$$c_m(t)a_m(t) = 0, \quad m \in \{1, 2, \dots, M\}. \quad (3)$$

Moreover, due to the multicast mechanism, we would not start multicasting the same message on more than one channel at the same time. That is,

$$a_m(t) \neq a_{m'}(t), \quad \text{if } a_m(t) > 0 \text{ and } m \neq m'. \quad (4)$$

3) *Transitions*: The transitions are to update *request matrix*, *channel availability*, and *channel status*. First, we define the *multicasting status* of the n^{th} message at the t^{th} time slot as

$$b_n(t) \triangleq \mathcal{I} \left(\sum_{m=1}^M \mathcal{I}_n(a_m(t)) \right), \quad n \in \{0, 1, \dots, N\}, \quad (5)$$

where $\mathcal{I}_n(x)$ equals 1 if x is n , and otherwise, equals 0. Apparently, $b_n(t)$ equals 1 if the n^{th} message is selected for multicasting over some channels in the beginning of the t^{th} time slot, and otherwise, it equals 0. Then, based on $b_n(t)$, the transitions are derived as follows.

Request matrix: We update the *request matrix* in the following two cases:

- If the n^{th} message is selected for multicasting in the beginning of the t^{th} time slot, i.e., $b_n(t) = 1$, only $q_n(t)$ new requests will be left in the request buffer in the beginning of the next time slot. Hence, $\mathbf{q}_n(t+1) = [q_n(t), 0, \dots, 0]^T$;
- If the n^{th} message is not selected for multicasting, the buffered requests in the beginning of the next time slot contain both the previously buffered ones and the newly arrived ones.

To summary, we have

$$\mathbf{q}_n(t+1) = \begin{cases} \left[q_n(t), \underbrace{0, \dots, 0}_{M^*-1 \text{ zeros}} \right]^T & b_n(t) = 1 \\ \left[q_n(t), [\mathbf{q}_n(t)^T]_{(1:M^*-2)}, [\mathbf{q}_n(t)]_{M^*-1} \right. \\ \left. + [\mathbf{q}_n(t)]_{M^*} \right]^T & b_n(t) = 0. \end{cases} \quad (6)$$

where $[\mathbf{q}_n(t)^T]_{1:M^*-2}$ is the 1-by- (M^*-2) -dimension vector containing the first to the $(M^*-2)^{\text{th}}$ entries of $\mathbf{q}_n(t)^T$.

Channel availability: We update the *channel availability* in the following three cases:

- If the m^{th} channel has been reserved for multicasting the n^{th} message in previous slots, i.e., $c_m(t) > 0$. The remaining time for the release of the m^{th} channel decreases by one in the beginning of the next time slot, i.e., $c_m(t+1) = c_m(t) - 1$;
- If the m^{th} channel has not been reserved for multicasting the n^{th} message and is going to multicast the n^{th} message in the beginning of the t^{th} time slot, i.e., $c_m(t) = 0$ and $a_m(t) = n$, the m^{th} channel will be released after $T_{n,m} - 1$ time slots counting from the $(t+1)^{\text{th}}$ time slot, i.e., $c_m(t+1) = T_{n,m} - 1$;
- If the m^{th} channel has not been reserved for multicasting the n^{th} message and is not going to multicast any message, i.e., $c_m(t) = 0$ and $a_m(t) = 0$, $c_m(t+1)$ remains 0.

To summary, we have

$$c_m(t+1) = \begin{cases} c_m(t) - 1 & c_m(t) > 0 \\ T_{n,m} - 1 & c_m(t) = 0, a_m(t) = n \\ 0 & c_m(t) = 0, a_m(t) = 0. \end{cases} \quad (7)$$

Channel status: Based on (1), (2), and (6), it can be derived that

$$g_{n,m}(t+1) = \begin{cases} \min_{q \in \{1, \dots, q_n(t)\}} \{g_{n,m,q}(t)\} & b_n(t)=1 \\ \min\{g_{n,m}(t), \min_{q \in \{1, \dots, q_n(t)\}} \{g_{n,m,q}(t)\}\} & b_n(t)=0, \end{cases} \quad (8)$$

where $g_{n,m,q}(t)$ is considered to be i.i.d. with respect to q and t , implying that MUs requesting different messages are identically distributed and send requests following a Poisson distribution.

4) *Reward:* Both the energy consumption and the latency penalty are the concerned performance metrics.

Energy consumption: The energy consumption of multicasting the n^{th} message over the m^{th} channel within the t^{th} time slot is $\frac{Z_{n,m}}{g_{n,m}(t)}$ [24], where $Z_{n,m} = \tau \left(2^{\frac{C}{\tau B}} - 1\right)$ is a constant with C , B , and τ being the information bits of the n^{th} message to be transmitted within one time slot, the bandwidth of the m^{th} channel, and the duration of one time slot, respectively. Accordingly, the total energy consumption of the multicast transmissions starting from the t^{th} time slot is computed as $\sum_{n=1}^N \sum_{m=1}^M \frac{T_{n,m} Z_{n,m}}{g_{n,m}(t)} \mathcal{I}_n(a_m(t))$.

Latency penalty: The requests buffered at the BS will produce instant latency penalty in every time slot before they get served. Denote a function $p_n(\tau) \in \mathbb{R}$ as the instant latency penalty for delaying one request for the n^{th} message over τ time slots. Then, according to (1), the buffered requests in $\mathbf{q}_n(t)$ will produce instant latency penalty of $\sum_{\tau=1}^{M^*} [\mathbf{q}_n(t)]_{\tau} p_n(\tau)$ at the t^{th} time slot. Thus, the total instant latency penalty produced at the t^{th} time slot is $\sum_{n=1}^N \sum_{\tau=1}^{M^*} [\mathbf{q}_n(t)]_{\tau} p_n(\tau)$.

The reward $r(t)$ of the considered system is defined as the weighted sum of the energy consumption and the latency penalty, i.e.,

$$r(t) \triangleq - \left(V \sum_{n=1}^N \sum_{m=1}^M \frac{T_{n,m} Z_{n,m}}{g_{n,m}(t)} \mathcal{I}_n(a_m(t)) + \sum_{n=1}^N \sum_{\tau=1}^{M^*} [\mathbf{q}_n(t)]_{\tau} p_n(\tau) \right), \quad (9)$$

where $V > 0$ is the tradeoff parameter.

5) *Problem formulation:* We aim to minimize the long-term average reward and thus formulate the multicast scheduling problem as

$$\begin{aligned}
 \text{(P1)} \quad & \max_{\{\mathbf{a}(t)\}} \lim_{T \rightarrow \infty} \mathbb{E}_{\{q_n(t)\}, \{g_{n,m,q}(t)\}} \left[\frac{1}{T} \sum_{t=1}^T r(t) \right] \\
 \text{s.t.} \quad & (3), (4), (6), (7), (8),
 \end{aligned} \tag{10}$$

where the expectation is taken with respect to the request arrival process $\{q_n(t)\}$ and the channel gain process $\{g_{n,m,q}(t)\}$.

Remark 2.1: There are three challenges in Problem (P1): large state space; large discrete action space; and time-varying and time-invariant constraints for the actions in (3) and (4).

- *The first challenge cannot be addressed by conventional dynamic programming, since solving the Bellman optimality equation requires significant computational resources when the state space is large [22].*
- *Modern deep reinforcement learning (DRL) algorithms cannot efficiently solve the MDPs with large discrete action space because the scale of the required policy network by DRL in this case becomes prohibitively large, which poses significant challenges for the convergence to the optimal solution. To alleviate this challenge, existing works proposed three techniques: (1) The first technique is to convert the discrete-valued action to a one-hot action. The output of DRL's policy network is then used to denote the values of the one-hot vector. However, this method becomes impractical when the dimension or domain of the original action space increases, since it results in an explosion of the dimensionality of the one-hot vector. (2) The second approach, known as action-embedding, uses DDPG to output a continuous-valued action of the same dimensionality as the original action space. Then, this approach selects several discrete-valued actions near the continuous-valued action as candidate actions and picks the best-evaluated one among them as the action. However, this approach may suffer from unstable convergence and poor performance when the action space is large. (3) The last approach is multi-agent DRL (MADRL), which uses individual policy networks to determine the action value on each dimension. This approach has promising performance and does not suffer from the large discrete action space issue. However, it cannot deal with the constraints on the action space.*
- *Both time-varying and time-invariant constraints are difficult to handle for DRL or MADRL*

algorithms, as their trial-and-error mechanism makes it challenging to avoid visiting actions that violate the constraints. In [23], the authors proposed a novel MADRL-based algorithm, which modifies the policy network structure and can efficiently address the time-varying constraints issue in a large discrete action space. However, it remains an open problem to solve MDPs with time-invariant constraints, when the action space is large and discrete.

To address the aforementioned challenges, we propose to transform problem **(P1)** into an equivalent Markov game **(P2)** by treating each channel as an individual agent. This approach allows us to employ the MADRL algorithm to obtain the optimal policy. The components of **(P2)** are specified as follows:

- **Agent observation:** The m^{th} agent's observation is denoted as $\mathbf{s}_m(t) \triangleq (\mathbf{Q}(t), c_m(t), \mathbf{g}_m(t))$, where $\mathbf{g}_m(t) \triangleq [g_{1,m}(t), \dots, g_{N,m}(t)]^T$ represents the channel gains for multicasting M messages over the m^{th} channel. Thus, the observation space has dimensionality of $NM^* + 1 + N$;
- **Agent action:** The m^{th} agent's action is $a_m(t)$;
- **Agent reward:** The reward for each agent is $r(t)$.

and the equivalence between **(P1)** and **(P2)** can be proven using similar method as that in [23] and thus is omitted for simplicity. To handle the time-varying and time-invariant constraints, we propose a modified MADRL algorithm, which will be discussed in details in the next section.

III. DISTRIBUTION-EMBEDDING MULTI-AGENT PROXIMAL POLICY OPTIMIZATION

This section introduces DE-MAPPO, an innovative algorithm that not only facilitates the efficient multicasting of multiple messages over multiple channels, but also guarantees that the chosen actions satisfy both the time-varying and time-invariant constraints. The algorithm consists of multiple modified proximal policy optimization (PPO) modules and a distribution-embedding (DE) module. Each modified PPO module is responsible for the scheduling over one channel and generates a distribution that contains the probabilities of multicasting different messages over this particular channel. The generated distribution is designed to satisfy the time-varying constraints in (3). The DE module integrates the distributions generated by all modified PPO modules to determine the channel schedule decision that satisfies the time-invariant constraints in (4).

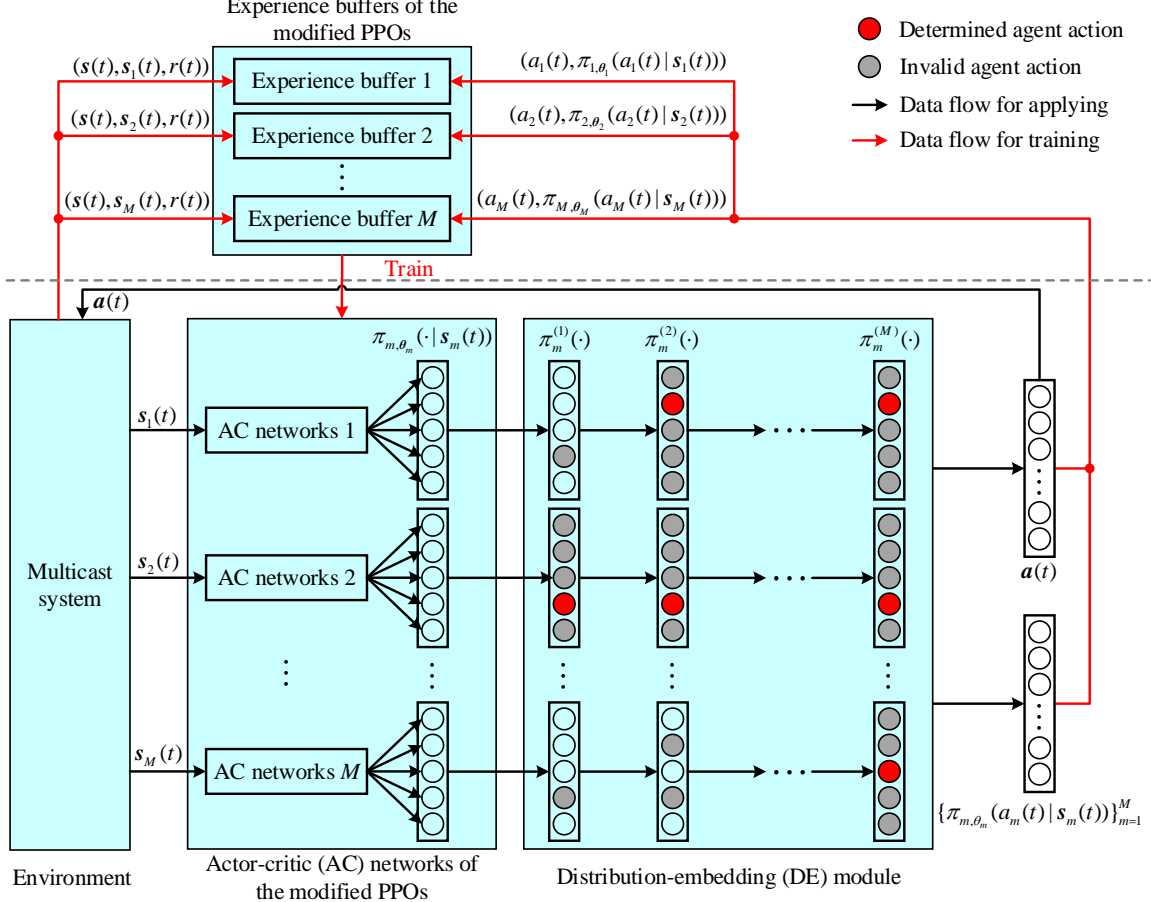


Figure 2: Structure of the proposed DE-MAPPO.

In the following, we first describe the structure of the proposed algorithm. Then, we present the offline training algorithm and the online validation algorithm to solve problem **(P1)**.

A. Structure of proposed algorithm

The proposed algorithm consists of M modified PPO modules and an DE module.

1) *Modified PPOs*: The m^{th} modified PPO is responsible for scheduling the m^{th} channel and denoted as PPO_m . As illustrated in Fig. 2, PPO_m contains an actor-critic (AC) network and an experience buffer, and the AC network consists of an actor network and a critic network.

- **Actor network**: The actor network of PPO_m is a fully connected neural network (NN) parameterized by θ_m and denoted as π_{m, θ_m} . It takes $s_m(t)$ as input, resulting in $NM^* + 1 + N$ nodes at the input layer. Its output layer consists of $N + 1$ nodes that correspond to the $N + 1$ possible agent actions, including multicasting no message, multicasting the 1st message,

multicasting the 2nd message, and so on up to multicasting the N^{th} message. Each node generates a value that represents the probability of selecting the corresponding agent action. Finally, we adopt $\{\pi_{m,\theta_m}(a|\mathbf{s}_m(t))\}_{a=0}^N$ to refer to the probabilities generated by the actor network of PPO _{m} and $\pi_{m,\theta_m}(\cdot|\mathbf{s}_m(t))$ to the corresponding action distribution, respectively. Remarkably, if the m^{th} channel is currently unavailable, i.e., $c_m(t) = 1$, the corresponding agent action $a_m(t)$ must be 0 based on the time-varying constraint in (3). In such cases, we manually adjust the agent action distribution $\pi_{m,\theta_m}(\cdot|\mathbf{s}_m(t))$ as

$$\pi_{m,\theta_m}(a|\mathbf{s}_m(t)) = \begin{cases} 1 & a = 0 \text{ and } c_m(t) = 1 \\ 0 & a > 0 \text{ and } c_m(t) = 1. \end{cases} \quad (11)$$

- **Critic network:** The critic network of PPO _{m} is also a fully connected NN, which is parameterized by ϕ_m and denoted as V_{m,ϕ_m} . It takes $\mathbf{s}(t)$ as input and thus has $NM^* + M + NM$ nodes at the input layer. Its output layer has only one node and generates the value function [25] of the state $\mathbf{s}(t)$, which is denoted as $V_{m,\phi_m}(\mathbf{s}(t))$;
- **Experience buffer:** The experience buffer of PPO _{m} stores the generated experiences during the offline training phase, which are the five-component tuples $(\mathbf{s}(t), \mathbf{s}_m(t), r(t), a_m(t), \pi_{m,\theta_m}(a_m(t)|\mathbf{s}_m(t)))$.

Remark 3.1: Compared to the conventional PPO, the modified PPO adopted in the proposed algorithm modifies the output of the actor network as shown in (11), which effectively prevents the exploration of infeasible actions that violate the time-varying constraints in (3). Remarkably, this modification has been validated to have no negative impact on the convergence performance of PPO [23].

2) *DE module:* The DE module integrates the output distributions of M modified PPOs, represented by $\{\pi_{m,\theta_m}(\cdot|\mathbf{s}_m(t))\}_{m=1}^M$, to determine the action value $\mathbf{a}(t)$. The integration process consists of several steps. First, stochastic agent ordering is utilized to determine the sequence in which each agent selects its agent action. Then, agent action selection and distribution modification are performed iteratively for M rounds, each of which determines the action for a specific agent. Finally, after the M iterations, agent action integration is performed to combine the values of all the agent actions and produce the final output $\mathbf{a}(t)$. To provide a more comprehensive explanation, we elaborate on each step with more details as follows:

- **Stochastic agent ordering:** In this step, we randomly permute vector $[1, 2, \dots, M]^T$ to generate a random permutation $\mathbf{u}(t) \in \{1, 2, \dots, M\}^{M \times 1}$, i.e.,

$$\mathbf{u}(t) = \text{Perm}([1, 2, \dots, M]^T), \quad (12)$$

where $\text{Perm}(\mathbf{x})$ is a function to generate a random permutation of vector \mathbf{x} . The elements of $\mathbf{u}(t)$ determine the order in which each agent takes action. Specifically, we denote the m^{th} element of $\mathbf{u}(t)$ as $u_m(t)$. Then, the m^{th} agent action selection determines the agent action of the $u_m(t)^{\text{th}}$ agent.

- **m^{th} agent action selection:** In this step, we determine the value of $a_{u_m(t)}(t)$ by sampling a random value from distribution $\pi_{u_m(t)}^{(m-1)}(\cdot)$, i.e.,

$$\Pr\{a_{u_m(t)}(t)=a\} = \pi_{u_m(t)}^{(m-1)}(a), \forall a \in \{0, 1, \dots, N\}, \quad (13)$$

where $\{\pi_{m'}^{(m-1)}(\cdot)\}_{m'=1}^M$ are generated from the previous iteration of the distribution modification. Moreover, the initial distributions are defined as $\pi_{m'}^{(0)}(\cdot) \triangleq \pi_{m', \theta_{m'}}(\cdot | \mathbf{s}_{m'}(t))$ with $m' \in \{1, 2, \dots, M\}$.

- **m^{th} distribution modification:** In this step, we generate new distributions $\pi_{m'}^{(m)}(\cdot)$ for all $m' \in \{u_{\hat{m}}(t) | \hat{m} > m\}$. First, for all $m' \in \{u_{\hat{m}}(t) | \hat{m} > m\}$, we use temporary distributions $\hat{\pi}_{m'}(\cdot)$ to inherit the distributions from the previous iteration of the distribution modification, i.e.,

$$\hat{\pi}_{m'}(\cdot) = \pi_{m'}^{(m-1)}(\cdot), \forall m' \in \{u_{\hat{m}}(t) | \hat{m} > m\}. \quad (14)$$

Then, based on the fact that the $u_m(t)^{\text{th}}$ agent is to multicast the $a_{u_m(t)}(t)^{\text{th}}$ message and the other agents would not multicast this message again, we revise the temporary distributions by

$$\hat{\pi}_{m'}(a_{u_m(t)}(t)) = 0, \text{ if } a_{u_m(t)}(t) \neq 0, \quad (15)$$

for all $m' \in \{u_{\hat{m}}(t) | \hat{m} > m\}$. Finally, we normalize the temporary distributions $\{\hat{\pi}_{m'}(\cdot)\}_{m' \in \{u_{\hat{m}}(t) | \hat{m} > m\}}$ and assign them to $\{\pi_{m'}^{(m)}(\cdot)\}_{m' \in \{u_{\hat{m}}(t) | \hat{m} > m\}}$, i.e.,

$$\pi_{m'}^{(m)}(a) = \frac{\hat{\pi}_{m'}(a)}{\sum_{\hat{m}=1}^M \hat{\pi}_{\hat{m}}(a)}, \forall m' \in \{u_{\hat{m}}(t) | \hat{m} > m\}, a \in \{0, 1, \dots, N\}. \quad (16)$$

- **Agent actions integration:** In this step, we combine the agent actions selected in M iterations of the agent action selection to produce action $\mathbf{a}(t)$, where the value of $a_{u_m(t)}(t)$ with $u_m(t) \in \{1, 2, \dots, M\}$ is obtained in the m^{th} agent action selection round according to (13). Additionally, we collect the values of $\{\pi_{m,\theta_m}(a_m(t)|\mathbf{s}_m(t))\}_{m=1}^M$ for offline training purposes.

Remark 3.2: Each distribution modification updates the agent action distributions for agents who have not yet determined their agent actions. Using equations (14), (15), and (16), each agent can select agent action following a normalized version of the original PPO-generated distribution, excluding the distribution part involving already selected agent actions by other agents. This ensures that all selected agent actions satisfy the time-invariant constraints in (4). After the M iterations, we combine the selected agent actions to produce action $\mathbf{a}(t)$, which also satisfies these constraints.

B. Offline training

We first simulate an offline environment based on the historical observations on $\{q_n(t)\}$ and $\{g_{n,m,q}(t)\}$. Then, we iteratively generate experiences by interacting with this simulated environment and update the PPO parameters based on these experiences.

1) *Offline environment simulation:* Based on the statistical features of $\{q_n(t)\}$ and $\{g_{n,m,q}(t)\}$, we simulate an offline environment to provide the following functions.

- **State evolution:** We simulate $\{q_n(t)\}$ and $\{g_{n,m,q}(t)\}$ based on their statistical features and use them along with the current state $\mathbf{s}(t)$ to calculate the next state $\mathbf{s}(t+1)$ and the next agent observations $\{\mathbf{s}_m(t+1)\}_{m=1}^M$ with (6), (7), and (8).
- **Reward generation:** Reward $r(t)$ is calculated based on (9).

2) *Experience generation phase:* During this step, M modified PPOs interact with the offline environment to sequentially generate N_B experiences, where N_B is the size of the experience buffer. At the t^{th} time slot, we send the agent observations $\{\mathbf{s}_m(t)\}_{m=1}^M$ to M actor networks and derive the action distributions $\{\pi_{m,\theta_m}(\cdot|\mathbf{s}_m(t))\}_{m=1}^M$. We then send these distributions to the DE module to obtain the values of $\mathbf{a}(t)$ and $\{\pi_{m,\theta_m}(a_m(t)|\mathbf{s}_m(t))\}_{m=1}^M$. Next, we send $\mathbf{a}(t)$ to the simulated offline environment to obtain reward $r(t)$ and the next set of agent observations $\{\mathbf{s}_m(t+1)\}_{m=1}^M$. We repeat the above procedures for N_b iterations from the t^{th} time slot to the

$t + N_B - 1$ time slot. We pack the related information into M sets of experiences, where the m^{th} set is denoted as

$$\{(\mathbf{s}(t), \mathbf{s}_m(t), a_m(t), r(t), \pi_{m, \theta_m}(a_m(t) | \mathbf{s}_m(t)))\}_t^{t+N_B-1},$$

and store it in the experience buffer at PPO_m .

3) *PPO update phase*: After each experience generation phase, we perform N_U update iterations on the parameters of the M modified PPOs. At the beginning of each update, we denote the actor and critic networks for PPO_m at that moment as π'_m and V'_m , respectively. Next, we estimate the value functions, advantage functions, and probability ratios for PPO_m as

$$V_m(t') = r(t') + \alpha r(t'+1) + \dots + \alpha^{N_B-1} r(t'+N_B-1), \quad (17)$$

$$A_m(t') = V_m(t') - V'_m(\mathbf{s}(t')), \quad (18)$$

$$R_m(t') = \begin{cases} 1 & b_m(t') > 0 \\ \frac{\pi'_m(a_m(t') | \mathbf{s}_m(t'))}{\pi_{m, \theta_m}(a_m(t') | \mathbf{s}_m(t'))} & b_m(t') = 0, \end{cases} \quad (19)$$

for all $t' \in \{t, t+1, \dots, t+N_B-1\}$, respectively [23]. Then, the surrogate loss for PPO_m is computed as

$$\begin{aligned} L_m = \sum_{t'=t}^{t+N_B-1} \frac{1}{N_B} & \left(- \min(R_m(t') A_m(t'), \right. \\ & \left. \text{clip}(R_m(t'), 1 - \epsilon, 1 + \epsilon) A_m(t')) \right. \\ & \left. + c_1 A_m(t')^2 - c_2 H(\pi'_m(\cdot | \mathbf{s}_m(t'))) \right), \end{aligned} \quad (20)$$

where $\text{clip}(x, a, b) \triangleq \min(\max(x, a), b)$ clamps x into the area $[a, b]$; $H(\pi'_m(\cdot | \mathbf{s}_m(t)))$ is the entropy of the distribution $\pi'_m(\cdot | \mathbf{s}_m(t))$; and ϵ , c_1 , and c_2 are some constants. Finally, we use this surrogate loss to update both the actor and critic networks via back propagations [26].

Remarkably, the experience generation phase and PPO update phase are executed alternately during the offline training. The entire offline training algorithm is summarized in Algorithm I.

C. Online applying

The online application algorithm is similar to the offline training one and the main difference between them is that the online one does not store the generated experiences or execute the PPO

Algorithm I Offline training algorithm for multicast schedule

- 1: Initialize the AC networks for M modified PPOs with random parameters $\{\boldsymbol{\theta}_m\}_{m=1}^M$ and $\{\boldsymbol{\phi}_m\}_{m=1}^M$;
 - 2: Define the maximum channel gain as $L \triangleq \max_{n,m,q,t} g_{n,m,q}(t)$;
 - 3: Set the value of the maximum learning episode L_E to a large integer;
 - 4: Initialize an experience buffer for each modified PPO;
 - 5: Simulate the offline environment according to Section III-B1;
 - 6: **for** episode= 1, 2, \dots , L_E
 - 7: Let $\mathbf{Q}(1) = 0^{N \times M^*}$, $\mathbf{c}(1) = \mathbf{0}^{M \times 1}$, $\mathbf{G}(1) = L^{N \times M}$;
 - 8: Derive $\{\mathbf{s}_m(1)\}_{m=1}^M$ by $\mathbf{s}_m(1) = (\mathbf{Q}(1), \mathbf{c}_m(1), \mathbf{g}_m(1))$;
 - 9: **for** $t = 1, 2, \dots, N_B$
 - 10: Send $\{\mathbf{s}_m(t)\}_{m=1}^M$ to M modified PPOs and derive $\{\pi_{m,\boldsymbol{\theta}_m}(\cdot|\mathbf{s}_m(t))\}_{m=1}^M$ based on (11);
 - 11: Send $\{\pi_{m,\boldsymbol{\theta}_m}(\cdot|\mathbf{s}_m(t))\}_{m=1}^M$ to the DE module and derive $\mathbf{a}(t)$ and $\{\pi_{m,\boldsymbol{\theta}_m}(a_m(t)|\mathbf{s}_m(t))\}_{m=1}^M$ based on (12), (13), (14), (15), and (16);
 - 12: Send $\mathbf{a}(t)$ to the simulated offline environment and derive $r(t)$ and $\{\mathbf{s}_m(t+1)\}_{m=1}^M$ based on (6), (7), (8), and (9);
 - 13: Store $\{(\mathbf{s}(t), \mathbf{s}_m(t), a_m(t), r(t), \pi_{m,\boldsymbol{\theta}_m}(a_m(t)|\mathbf{s}_m(t)))\}_{t=1}^{N_B}$ in the experience buffer of PPO $_m$;
 - 14: **end for**
 - 15: **for** iteration= 1, 2, \dots , N_U
 - 16: **for** $m = 1, 2, \dots, M$
 - 17: Load the stored experiences;
 - 18: Calculate the surrogate loss L_m based on (17), (18), (19), and (20);
 - 19: Update $\boldsymbol{\theta}_m$ and $\boldsymbol{\phi}_m$ by backpropagating L_m ;
 - 20: **end for**
 - 21: **end for**
 - 22: Empty all the experience buffers;
 - 23: **end for**
 - 24: **end for**
-

update in lines 13-20 of Algorithm I. Additionally, the agent observations are derived directly from the real environment, not the simulated one.

Remark 3.3: The relationships between conventional DRL, the action-embedding method, and the proposed distribution-embedding method are summarized as follows.

- *Conventional DRL algorithms directly determine the action value based on the output of their actor networks, while the action-embedding and distribution-embedding methods send*

the output of the actor network to an additional module that determines the action value. By doing so, it is unnecessary to encode the action as a high-dimensional one-hot vector to satisfy the requirement for conventional DRL algorithms, which not only reduces the scale of the NN but also enhances convergence performance of DRL.

- *The action-embedding method uses an additional module to generate multiple candidate actions based on the suggested action by DRL and selects the one with the optimal estimated evaluation as the final action. However, this method has limitations for MDPs with large discrete action spaces and time-varying, time-invariant constraints. To elaborate, the method proposed in [27] relies on DDPG training mechanism and generates candidate actions with a poorly interpretive approach, limiting its performance for the cases with large discrete action spaces. On the other hand, the method proposed in [28] achieves promising results but is limited to scenarios with binary-valued high-dimensional action spaces. Moreover, both methods fail to handle the cases with time-varying or time-invariant constraints due to the high possibility of generating infeasible candidate actions. A possible solution to this issue is to generate a large number of candidate actions, hoping to find feasible ones, while this approach requires an unstable number of trials and could be problematic for the cases with high-dimensional action spaces. Additionally, if generating one feasible candidate action consumes too many trials, this approach can degrade into a purely random policy, rendering the action suggested by the original DRL irrelevant.*
- *The proposed distribution-embedding method can efficiently handle the challenges of time-invariant constraints. It iteratively modifies the action distribution suggested by MADRL and determines the value of action dimension-by-dimension, ensuring that the final action follows an action distribution similar to the one generated by MADRL and satisfies the time-invariant constraints. Finally, by combining the distribution-embedding method with the modified MAPPO, the proposed DE-MAPPO achieves better performance than the existing methods in scenarios with large discrete action space and time-varying, time-invariant constraints.*

IV. DISCUSSION

In this section, we derive the upper bound of the objective function of problem **(P1)**, and it works as the benchmark to validate the proposed DE-MAPPO in the simulation part. To derive the upper bound, we first relax the time-varying constraints of problem **(P1)** in (3) to a

set of time-invariant constraints, which reveal the statistical features of any multicast schedule policy satisfying the constraints in (3). Then, we convert the relaxed problem to a two-step optimization problem, where the optimization of the first step purely minimizes the latency penalty and the second step jointly minimizes the energy consumption and the latency penalty. Finally, we successively analyze the optimizations of these two steps, and obtain an upper bound for problem **(P1)**.

1) *Constraints relaxation:* We can relax the time-varying constraints in (3) using the following proposition.

Proposition 4.1: For any multicast schedule policy satisfying the constraints in (3), it follows

$$\sum_{n=1}^N \gamma_{n,m}(T) T_{n,m} \leq T, \quad m \in \{1, 2, \dots, M\}, \quad T \in \mathbb{Z}^+, \quad (21)$$

where $\gamma_{n,m}(T) \in \mathbb{N}$ counts how many times the n^{th} message has been multicasting over the m^{th} channel from the 1^{st} to T^{th} time slots and is defined as

$$\gamma_{n,m}(T) \triangleq \sum_{t=1}^T \mathcal{I}_n(a_m(t)), \quad (22)$$

with $n \in \{1, 2, \dots, N\}$, $m \in \{1, 2, \dots, M\}$, and $T \in \mathbb{Z}^+$.

Sketch of the proof: If a multicast schedule policy satisfies the constraints in (3), then $\gamma_{n,m}(T)$ times of multicasting of the n^{th} message over the m^{th} channel would occupy the m^{th} channel for $\gamma_{n,m}(T) T_{n,m}$ time slots. As a result, all multicastings of N messages over the m^{th} channel would occupy the m^{th} channel for $\sum_{n=1}^N \gamma_{n,m}(T) T_{n,m}$ time slots, which must not exceed T . ■

Proposition 4.1 implies that the constraints in (21) are less restrictive than those in (3). Thus, we can simplify problem **(P1)** by replacing the constraints in (3) with those in (21). This results in a new problem **(P3)**:

$$\begin{aligned} \text{(P3)} \quad & \max_{\{\mathbf{a}(t)\}} \lim_{T \rightarrow \infty} \mathbb{E}_{\{q_n(t)\}, \{g_{n,m,q}(t)\}} \left[\frac{1}{T} \sum_{t=1}^T r(t) \right] \\ & \text{s.t.} \quad (6), (8), (21), \end{aligned}$$

where we drop the transitions in (7) since they are no longer needed without the constraints in (3). Additionally, we eliminate the constraints in (4) to further relax the problem.

2) *Problem conversion:* We convert problem **(P3)** to a two-step optimization problem. First, we let $\gamma_{n,m}(T)$ equal $\hat{\gamma}_{n,m}$ for all $n \in \{1, 2, \dots, N\}$, $m \in \{1, 2, \dots, M\}$, and $T \in \mathbb{Z}^+$, where $\hat{\gamma}_{n,m}$ is an integer in $\{0, 1, \dots, T\}$. Next, we only optimize the latency penalty term of problem **(P3)** by solving the following problem:

$$\begin{aligned} \text{(P4)} \quad & \max_{\{\mathbf{a}(t)\}} -\lim_{T \rightarrow \infty} \mathbb{E}_{\{q_n(t)\}} \left[\frac{1}{T} \sum_{t=1}^T \sum_{n=1}^N \sum_{\tau=1}^{M^*} [\mathbf{q}_n(t)]_{\tau} p_n(\tau) \right] \\ \text{s.t.} \quad & (6), \gamma_{n,m}(T) = \hat{\gamma}_{n,m}, n \in \{1, \dots, N\}, m \in \{1, \dots, M\}. \end{aligned}$$

Denote the upper bound of problem **(P4)** as $f(\hat{\gamma})$, where $\hat{\gamma}$ is a N -by- M -dimension matrix and defined by $[\hat{\gamma}]_{(n,m)} \triangleq \hat{\gamma}_{n,m}$. Then, we jointly optimize the energy consumption and the latency penalty terms of problem **(P3)** by further solving the following problem:

$$\begin{aligned} \text{(P5)} \quad & \max_{\{\mathbf{a}(t)\}, \hat{\gamma}} -V \lim_{T \rightarrow \infty} \mathbb{E}_{\{g_{n,m,q}(t)\}} \left[\frac{1}{T} \sum_{t=1}^T \sum_{n=1}^N \sum_{m=1}^M \frac{T_{n,m} Z_{n,m}}{g_{n,m}(t)} \right. \\ & \left. \mathcal{I}_n(a_m(t)) \right] + f(\hat{\gamma}) \\ \text{s.t.} \quad & (8), \\ & \sum_{n=1}^N \hat{\gamma}_{n,m} T_{n,m} \leq T, m \in \{1, 2, \dots, M\}, \end{aligned} \quad (23)$$

where the constraints in (23) is derived by (21). Since the optimal solutions to problems **(P4)** and **(P5)** may assign different values to the design variable $\{\mathbf{a}(t)\}$, problem **(P5)** is a relaxed version of problem **(P3)** and thus the upper bound of problem **(P5)** is also an upper bound of problem **(P3)**. In the following, we successively analyze problems **(P4)** and **(P5)** to derive the upper bound of problem **(P3)**.

3) *Upper bound of problem (P4):* By splitting both the objective function and the constraints of problem **(P4)**, we divide problem **(P4)** into N sub-problems, where the n^{th} sub-problem is given as

$$\text{(P4-1)} \quad \min_{\{\mathbf{a}(t)\}} -\lim_{T \rightarrow \infty} \mathbb{E}_{\{q_n(t)\}} \left[\frac{1}{T} \sum_{t=1}^T \sum_{\tau=1}^{M^*} [\mathbf{q}_n(t)]_{\tau} p_n(\tau) \right] \quad (24)$$

$$\text{s.t.} \quad (6),$$

$$\gamma_{n,m}(T) = \hat{\gamma}_{n,m}, m \in \{1, \dots, M\}. \quad (25)$$

Note that the optimal solutions to N sub-problems may assign different values to $\{\mathbf{a}(t)\}$. Thus, the summation of the optimal values of N sub-problems **(P4-1)** serves as an upper bound of problem **(P4)**.

Problem **(P4-1)** can be interpreted as: *If the number of the multicastings for the n^{th} message is fixed as $\sum_{m=1}^M \hat{\gamma}_{n,m}$ within the 1^{st} to T^{th} time slots, when should we start these multicastings to minimize the average latency penalty?* To solve this problem, let t_i , $i \in \{1, 2, \dots, \sum_{m=1}^M \hat{\gamma}_{n,m}\}$, denote the start time of the i^{th} multicasting. Without loss of generality, we set $t_{\sum_{m=1}^M \hat{\gamma}_{n,m}} = T$. Then, we rewrite the objective function of Problem **(P4-1)** as a summation of $\sum_{m=1}^M \hat{\gamma}_{n,m}$ individual terms, i.e.,

$$\begin{aligned} & \mathbb{E}_{\{q_n(t)\}} \left[\sum_{t=1}^T \sum_{\tau=1}^{M^*} [\mathbf{q}_n(t)]_{\tau} p_n(\tau) \right] \\ &= \sum_{i=1}^{\sum_{m=1}^M \hat{\gamma}_{n,m}} \mathbb{E}_{\{q_n(t)\}} \left[\sum_{t=t_{i-1}+1}^{t_i} \sum_{\tau=1}^{M^*} [\mathbf{q}_n(t)]_{\tau} p_n(\tau) \right] \end{aligned} \quad (26)$$

where the i^{th} term, $\mathbb{E}_{\{q_n(t)\}} \sum_{t=t_{i-1}+1}^{t_i} \sum_{\tau=1}^{M^*} [\mathbf{q}_n(t)]_{\tau} p_n(\tau)$, denotes the expected latency penalty incurred between the $(i-1)^{\text{th}}$ and i^{th} multicastings, and $t_0 \triangleq 0$ holds. Based on (6), the values of $\mathbf{q}_n(t)$ in any two of the $\sum_{m=1}^M \hat{\gamma}_{n,m}$ terms are independent. Thus, the optimal policy for problem **(P4-1)** only depends on the values of $\mathbf{q}_n(t)$ since the last multicasting. Let $\pi(\mathbf{q}_n(t)) \in \{0, 1\}$ denote the optimal decision for whether to start a new multicast based on the values of $\mathbf{q}_n(t)$ since the last multicasting. Then, problem **(P4-1)** can be rewritten as

$$\mathbf{(P4-2)} \quad \max_{\pi} -\mathbb{E}_{\pi, \{q_n(t)\}} \left[\sum_{t=1}^{t^*} \sum_{\tau=1}^{M^*} [\mathbf{q}_n(t)]_{\tau} p_n(\tau) \right]$$

s.t. (6),

$$[\mathbf{q}_n(1)]_1 \sim \text{Pois}(\lambda_n), \quad (27)$$

$$[\mathbf{q}_n(1)]_{(2:M^*)} = \mathbf{0}^{(M^*-1) \times 1}, \quad (28)$$

$$\mathbb{E}_{\pi, \{q_n(t)\}} t^* = \frac{T}{\sum_{m=1}^M \hat{\gamma}_{n,m}}. \quad (29)$$

In problem **(P4-2)**, we simulate the scenario where the last multicasting occurred at the 0^{th} time slot by initializing the value of $\mathbf{q}_n(1)$ as given in (27) and (28). The expression in (29) is derived from (25). Here, t^* represents the time at which to start a new multicasting given that the last

multicasting occurred at the 0th time slot, and it is defined as

$$t^* = \min\{t \in \mathbb{Z}^+ | \pi(\mathbf{q}_n(t)) = 1\}. \quad (30)$$

To solve problem **(P4-2)**, we use the vanilla DQN algorithm [29]. We first convert it into an MDP **(P4-3)** with the following components

- **State:** $\hat{\mathbf{s}}(t) \triangleq (\mathbf{q}_n(t), z(t))$;
- **Action:** $\hat{a}(t) \triangleq \pi(\mathbf{q}_n(t))$;
- **Transition:** (6) and

$$z(t+1) = \begin{cases} z(t) + 1 & \hat{a}(t) = 0 \\ z(t) - \frac{T}{\sum_{m=1}^M \hat{\gamma}_{n,m}} & \hat{a}(t) = 1; \end{cases}$$

- **Reward:** The reward at time t is defined as

$$\hat{r}(t) \triangleq \begin{cases} \sum_{\tau=1}^{M^*} [\mathbf{q}_n(t)]_{\tau} p_n(\tau) & \hat{a}(t) = 0 \\ \sum_{\tau=1}^{M^*} [\mathbf{q}_n(t)]_{\tau} p_n(\tau) - \left(z(t) - \frac{T}{\sum_{m=1}^M \hat{\gamma}_{n,m}} \right)^2 & \hat{a}(t) = 1. \end{cases}$$

Here, $z(t)$ calculates the value of t^* and $-\left(z(t) - \frac{T}{\sum_{m=1}^M \hat{\gamma}_{n,m}}\right)^2$ is added to the reward to ensure that the learned policy satisfies the constraints in (29). We then use a neural network to approximate the optimal policy, with $\hat{\mathbf{s}}(t)$ as the input and $q(\hat{\mathbf{s}}(t), \hat{a}(t))$ as the output. We train the network using the DQN algorithm, and estimate the optimal value of problem **(P4-2)**, i.e., $f(\hat{\gamma})$, using a long-term average evaluation on $\sum_{\tau=1}^{M^*} [\mathbf{q}_n(t)]_{\tau} p_n(\tau)$.

Particularly, for the case of $p_n(\tau) = 1$, it follows $\sum_{\tau=1}^{M^*} [\mathbf{q}_n(t)]_{\tau} p_n(\tau) = \sum_{\tau=1}^{M^*} [\mathbf{q}_n(t)]_{\tau}$, and we can simplify problem **(P4-2)** by defining $\bar{q}_n(t) \triangleq \sum_{\tau=1}^{M^*} [\mathbf{q}_n(t)]_{\tau}$, which represents the total number of stored requests for message n up to the t^{th} time slot. With this definition, we rewrite problem **(P4-2)** as

$$\begin{aligned} \text{(P4-3)} \quad & \max_{\bar{q}_n \in \mathbb{N}} -\mathbb{E}_{\{q_n(t)\}} \left[\sum_{t=1}^{t^*} \bar{q}_n(t) \right] \\ \text{s.t.} \quad & (29), \bar{q}_n(1) \sim \text{Pois}(\lambda_n), \\ & \bar{q}_n(t+1) = \begin{cases} q_n(t) & b_n(t) = 1 \\ \bar{q}_n(t) + q_n(t) & b_n(t) = 0 \end{cases}, \end{aligned} \quad (31)$$

where (31) is derived from (6). The optimal policy for problem **(P4-3)** can be validated to be a

threshold policy [18], where the time to start a new multicasting, denoted by t^* , is the smallest integer such that $\bar{q}_n(t^*) > \bar{q}_n$, i.e., $t^* = \min\{t \in \mathbb{Z}^+ | \bar{q}_n(t) > \bar{q}_n\}$. The optimal threshold value \bar{q}_n can be determined by using the optimal stopping rule [18]. Once this threshold value is found, the optimal value of problem **(P4-3)** can be calculated.

4) *Upper bound of problem (P5)*: Denote the minimum energy consumption to multicast the n^{th} message over the m^{th} channel as $e_{n,m}$, i.e.,

$$e_{n,m} \triangleq \frac{T_{n,m} Z_{n,m}}{\max_t g_{n,m}(t)}.$$

Then, based on the definition of $\gamma_{n,m}(T)$ in (22), it follows

$$\begin{aligned} & -V \lim_{T \rightarrow \infty} \mathbb{E}_{\{g_{n,m,q}(t)\}} \left[\frac{1}{T} \sum_{t=1}^T \sum_{n=1}^N \sum_{m=1}^M \frac{T_{n,m} Z_{n,m}}{g_{n,m}(t)} \mathcal{I}_n(a_m(t)) \right] \\ & \leq -V \lim_{T \rightarrow \infty} \frac{1}{T} \sum_{n=1}^N \sum_{m=1}^M e_{n,m} \gamma_{n,m}(T). \end{aligned}$$

Therefore, problem **(P5)** can be relaxed as

$$\begin{aligned} \text{(P5-1)} \quad & \max_{\gamma(T) \in \mathbb{N}^N \times M} -V \lim_{T \rightarrow \infty} \frac{1}{T} \sum_{n=1}^N \sum_{m=1}^M e_{n,m} \gamma_{n,m}(T) + f(\gamma(T)) \\ & \text{s.t.} \quad (21), \end{aligned}$$

where $\gamma(T)$ is defined by $[\gamma(T)]_{(n,m)} \triangleq \gamma_{n,m}(T)$. Problem **(P5-1)** can be solved by using integer programming [30] or the Lagrange multiplier technique by reforming the random variable as $\bar{\gamma}_{n,m} \triangleq \frac{\gamma_{n,m}(T)}{T} \in [0, 1]$. Then, the derived optimal value of problem **(P5-1)** is an upper bound of the objective function of problem **(P1)**.

V. SIMULATIONS AND NUMERICAL RESULTS

This section presents the performance evaluation of the proposed DE-MAPPO algorithm and compares it with state-of-the-art algorithms, including

- Optimal stopping rule [18]: an optimal policy for the case with $N = 1$ and $M = 1$;
- Relative value iteration (RVI) [19]: an optimal policy solely optimizing the summation latency penalty for the case with $N = 2$ and $M > 1$;
- MAPPO [23]: a state-of-the-art DRL policy applicable for the multi-message and multi-channel case. It can also address the issue of time-varying constraints by utilizing (11)

and (19) in the offline training and online applying phases, while it is not able to handle time-invariant constraints.

- Wolpertinger policy (WP) [27]: another state-of-the-art DRL policy applicable for the multi-message and multi-channel case. It generates k candidate actions at each time slot and pick the one with the best evaluation as the final action;
- Solution to problem **(P5-1)** (abbreviated as Upper bound **(P5-1)**);
- Round-Robin (RR) [31]: a typical benchmark policy where M channels take turns to multicast N messages.

We set the simulation parameters as follows. Mean values of request arrivals for N messages are uniformly picked from the set $\{10, 11, \dots, 20\}$. Downlink channel gains $g_{n,m,q}(t)$ are modeled as i.i.d. random variables over n, m, q and t , and follow the uniform distribution over $\{100, 101, \dots, 110\}$. Constant $Z_{n,m}$ is set as 500 for all $n \in \{1, 2, \dots, N\}$ and $m \in \{1, 2, \dots, M\}$ and the size of the request buffer is set as $M^* = 4$. In the adopted PPO modules, we set $N_B = 1000$, $N_U = 10$, $\alpha = 0.9$, $\epsilon = 0.2$. The learning rate for the actor and critic networks are both set as 0.001.

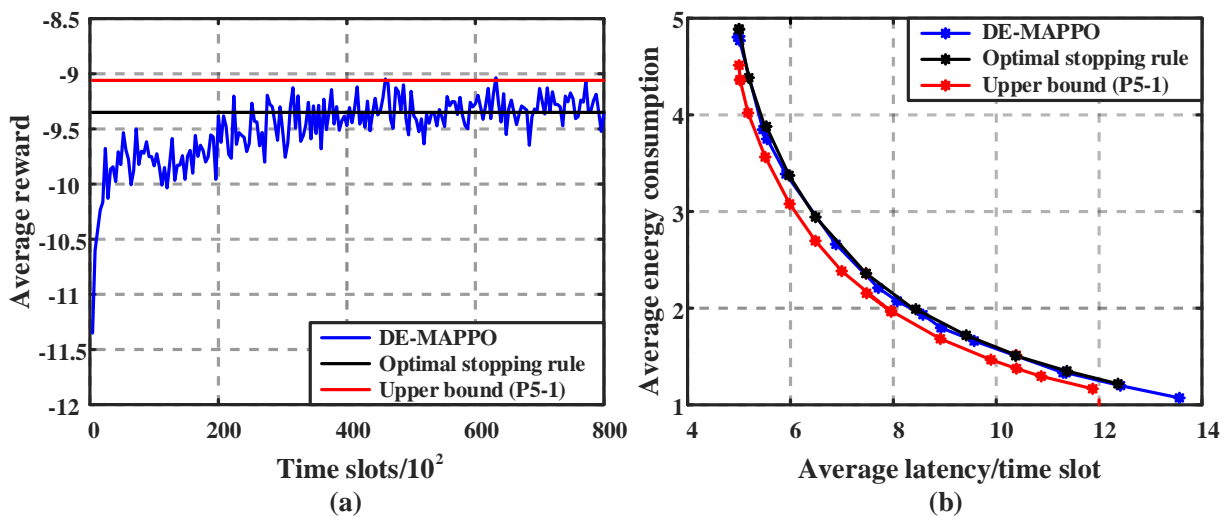


Figure 3: Performance comparison of DE-MAPPO with the benchmark algorithms for the scenario with $N = 1$ and $M = 1$. (a) average reward as a function of time slots in the offline training; (b) average latency vs. average energy consumption tradeoff.

In Fig. 3, we investigate the performances of DE-MAPPO, optimal stopping rule, and Upper bound **(P5-1)** in the scenario with one message and one channel, i.e., $N = 1$ and $M = 1$. Specifically, we consider the case that each multicasting of the message consumes 1 time slot,

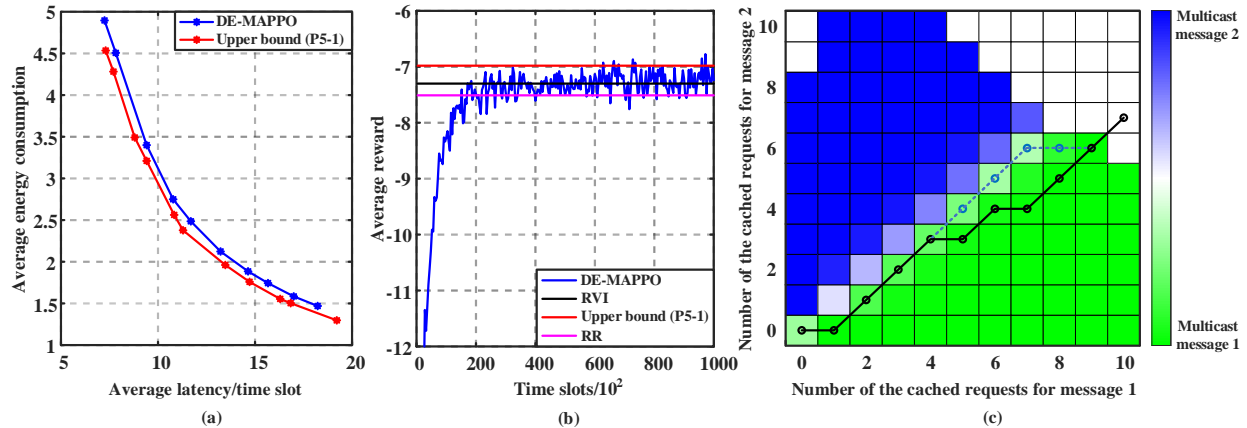


Figure 4: Performance comparison of DE-MAPPO with the benchmark algorithms for the scenario with $N = 2$, $M = 1$, and the size of the request buffers as 10. (a) average latency vs. average energy consumption tradeoff; (b) average reward as a function of time slots in the offline training; (c) schedule policy structure of DE-MAPPO and RVI.

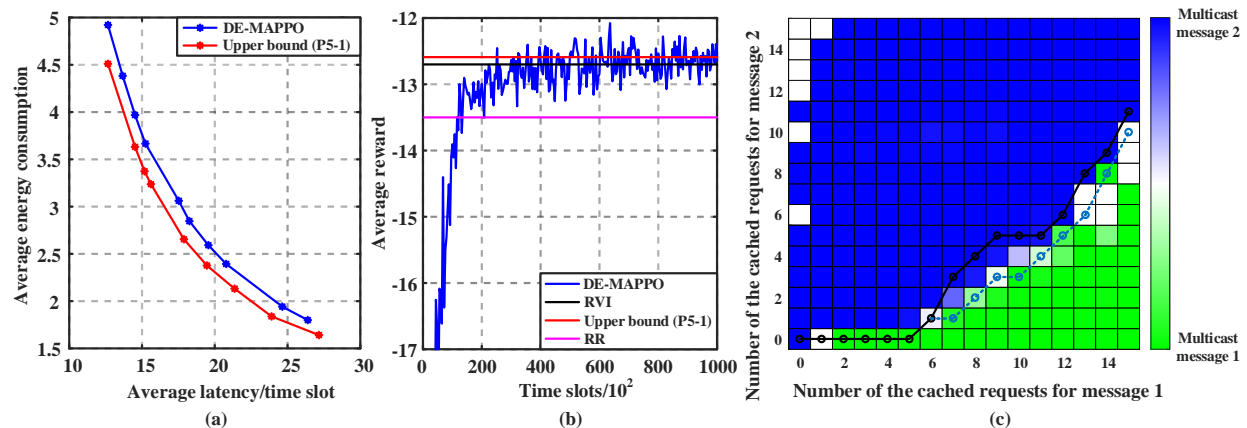


Figure 5: Performance comparison of DE-MAPPO with the benchmark algorithms for the scenario with $N = 2$, $M = 1$, and the size of the request buffers as 15. (a) average latency vs. average energy consumption tradeoff; (b) average reward as a function of time slots in the offline training; (c) schedule policy structure of DE-MAPPO and RVI.

i.e., $T_{1,1} = 1$, and let $p_1(\tau) = 1$ hold, such that the optimal stopping rule is applicable. Under this scenario, the proposed DE-MAPPO contains only one PPO module and can be validated to be exactly the pure PPO algorithm [26]. We adopt two-layer NNs for both the actor and critic networks of the PPO with each layer containing 16 nodes. Fig. 3(a) shows that DE-MAPPO converges after 40,000 time slots and achieves similar average reward compared to the optimal stopping rule method. To evaluate the tradeoff between average latency and average energy

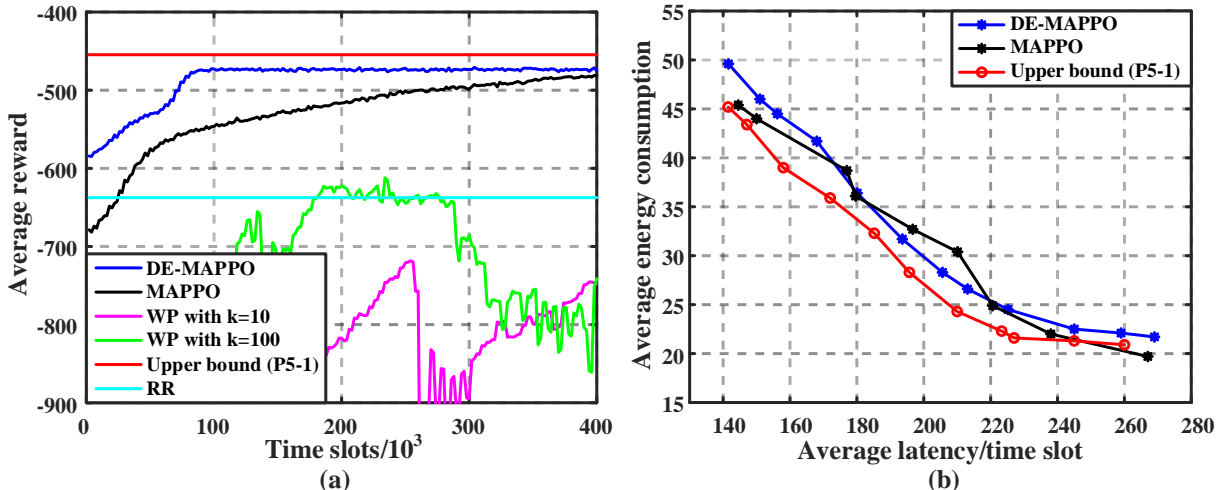


Figure 6: Performance comparison of DE-MAPPO with the benchmark algorithms for the scenario with $N = 10$ and $M = 10$. (a) average reward as a function of time slots in the offline training; (b) average latency vs. average energy consumption tradeoff.

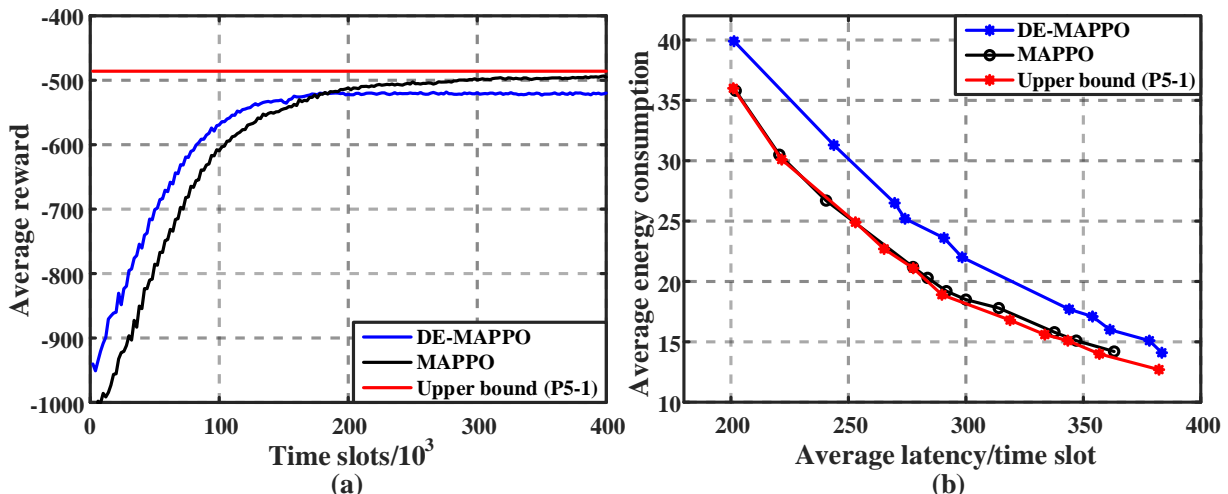


Figure 7: Performance comparison of DE-MAPPO with the benchmark algorithms for the scenario with $N = 10$, $M = 10$, $T_{n,m} = 1$, and $p_n(\tau) = 1$. (a) average reward as a function of time slots in the offline training; (b) average latency vs. average energy consumption tradeoff.

consumption achieved by different algorithms, we investigate their performances under various values of V and plot the corresponding tradeoff curves in Fig. 3(b). Numerical results show that both DE-MAPPO and the optimal stopping rule method achieve a slightly worse performance than Upper bound (P5-1). However, this is expected as Upper bound (P5-1) itself evaluates the upper bound performance of the optimal schedule policy.

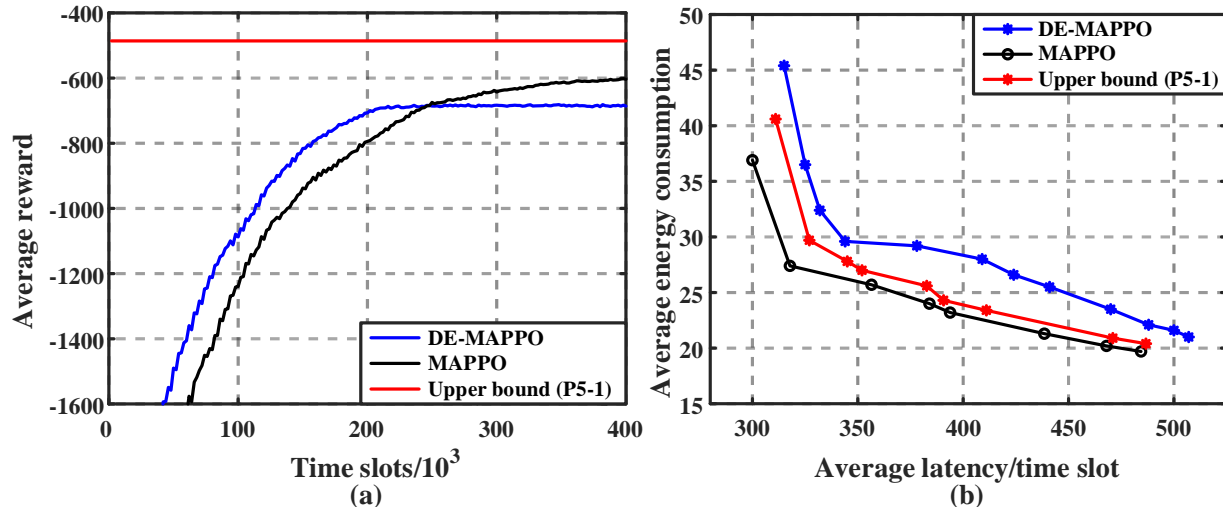


Figure 8: Performance comparison of DE-MAPPO with the benchmark algorithms for the scenario with $N = 10$, $M = 10$, $T_{n,m} = 1$, and $p_n(\tau) = \tau$. (a) average reward as a function of time slots in the offline training; (b) average latency vs. average energy consumption tradeoff.

Fig. 4 investigates the performances of DE-MAPPO, RVI, Upper bound (**P5-1**), and RR in the scenario with two messages and one channel, where the mean request arrival rates for the two messages are set as $\lambda_1 = 2$ and $\lambda_2 = 3$, respectively. To apply the RVI algorithm, we limit the size of the request buffer for both the messages as 10. The DE-MAPPO adopts two-layer NNs for both the actor and critic networks of the PPO, with each layer containing 32 nodes. Firstly, we evaluate the performance of DE-MAPPO under various values of V in Fig. 4(a), and we observe that DE-MAPPO again achieves a slightly worse performance than Upper bound (**P5-1**). Then, we set V to 0 and derive the policy that optimizes the summation latency penalty based on RVI. In Fig. 4(b), we observe that DE-MAPPO and RVI achieve similar average reward and outperform RR algorithm. Finally, Fig. 4(c) shows the structure of the schedule policy for DE-MAPPO and RVI under this scenario. The state of this scenario is a two-dimensional vector containing the numbers of cached requests for the two messages and plotted as squares in Fig. 4(c). At any state, the DE-MAPPO schedule policy is stochastic and uses a certain Bernoulli distribution to multicast two messages. Specifically, in states colored with deeper blue, DE-MAPPO assigns a higher probability of multicasting message 2, while in states colored with deeper green, it assigns a higher probability of multicasting message 1. In contrast, the optimal policy derived by RVI is deterministic and multicasts message 2 when the state lies above the plotted black curve and message 1 when the state lies on or below the curve. Both DE-MAPPO

and RVI showcase a switch-like behavior to determine which message to multicast, and their switch curves exhibit similarities.

Fig. 5 investigates the performances of the algorithms in a more complex scenario, where the mean request arrival rates for the two messages are $\lambda_1 = 2$ and $\lambda_2 = 7$, and the request buffer size for both messages is 15. The results obtained by DE-MAPPO are similar to those in Fig. 4, demonstrating its ability to achieve high rewards and a switch-like policy similar to RVI. However, it should be noted that obtaining the optimal policy using RVI requires evaluating the relative value over 256 states, which is a computationally intensive process. Moreover, the computational requirements would exponentially increase when extending RVI to the scenario with larger request buffer sizes or message numbers. In contrast, as shown in Fig. 4(b) and Fig. 5(b), the proposed DE-MAPPO can achieve comparable rewards to RVI with reasonable offline training times, which involve around 250 and 300 times of PPO parameter update, respectively. This highlights the advantages of DE-MAPPO over RVI in terms of computational efficiency.

Fig. 6 examines the performances of the algorithms in the scenario with 10 messages and 10 channels ($N = 10$ and $M = 10$), where the action space has a cardinality of 11^{10} and is too large for optimal stopping rule and RVI. In this setting, we compare DE-MAPPO with MAPPO, WP with $k = 10$ and $k = 100$, Upper bound **(P5-1)**, and RR algorithm. All DRL algorithms use three-layer NNs for both the actor and critic networks with 128 nodes per layer. As shown in Fig. 6(a), DE-MAPPO converges faster than MAPPO and achieves a similar average reward. The average reward of DE-MAPPO is also close to Upper bound **(P5-1)** and much higher than RR algorithm. WP algorithms do not converge well in this scenario due to its poorly interpretive training kernel that assumes actions close in Euclidean space yield similar rewards, which is not true in this case. Moreover, MAPPO is not able to restrict itself to selecting only feasible actions that satisfy the time-invariant constraints in (4), and instead optimizes the reward within a larger action space than the original MDP. As a result, MAPPO may achieve a higher reward than the optimal policy of the original MDP or even Upper bound **(P5-1)**. However, due to the same reason, MAPPO is actually not applicable in practice. Fig. 6(b) shows that DE-MAPPO has a tradeoff curve close to MAPPO and Upper bound **(P5-1)**, indicating its effectiveness in balancing the average latency and average energy consumption.

In Fig. 7, we investigate the performances of the algorithms in a more complex scenario, where the multicasting of each message over each channel may consume up to 5 time slots, i.e., $T_{n,m} \in \{1, 2, \dots, 5\}$. In this scenario, the schedule decision at each time slot must also

satisfy the time-varying constraints in (3). We evaluate various algorithms in Fig. 7(a), where WP and RR algorithms are not plotted since their performances are too bad. DE-MAPPO again converges faster than MAPPO and achieves comparable average reward to MAPPO and Upper bound (**P5-1**). In Fig. 7(b), the tradeoff curve of DE-MAPPO is again close to MAPPO and Upper bound (**P5-1**).

In Fig. 8, we consider the 10 messages and 10 channels case with a linear latency penalty function of $p_n(\tau) = \tau$. The results are similar to those in Fig. 7, which demonstrates the effectiveness of DE-MAPPO in scenarios with a general latency penalty function.

VI. CONCLUSIONS

We consider the multicast scheduling problem for multiple messages over multiple channels, which jointly optimizes the energy efficiency and the average latency penalty. This problem is formulated as an infinite-horizon MDP, which is challenging due to the large discrete action space, multiple time-varying constraints, and multiple time-invariant constraints. To address the first two issues, the modified MAPPO structure proposed in [23] is adopted. To address the time-invariant issue, a novel distribution-embedding approach is proposed, which iteratively modifies the output distribution of MAPPO and outperforms the existing action-embedding approaches. Finally, the structure of the considered MDP is analyzed, and a performance upper bound is derived by solving a two-step optimization problem.

REFERENCES

- [1] R. Li, C. Huang, H. Zhang, and S. Jiang, "Multicast schedule for multi-message over multi-channel: A permutation-based wolpertinger deep reinforcement learning method," in *Proc. IEEE ICC*, Foshan, China, Sep. 2022, pp. 826–831.
- [2] Zippia, "20 vital smartphone usage statistics [2023]: Facts, data, and trends on mobile use in the U.S." Available: <https://www.zippia.com/advice/smartphone-usage-statistics/>, Oct. 2022.
- [3] Ericsson, "Ericsson mobility report," Available: <https://www.ericsson.com/491da6/assets/local/reports-papers/mobility-report/documents/2022/ericsson-mobility-report-q4-2022.pdf>, Feb. 2023.
- [4] A. Biazon and M. Zorzi, "Multicast via point to multipoint transmissions in directional 5G mmwave communications," *IEEE Commun. Mag.*, vol. 57, no. 2, pp. 88–94, Feb. 2019.
- [5] Z. Li, C. Qi, and G. Y. Li, "Low-complexity multicast beamforming for millimeter wave communications," *IEEE Trans. Veh. Technol.*, vol. 69, no. 10, pp. 12 317–12 320, Oct. 2020.
- [6] Y. Li, M. Xia, and Y.-C. Wu, "Energy-efficient precoding for non-orthogonal multicast and unicast transmission via first-order algorithm," *IEEE Trans. Wireless Commun.*, vol. 18, no. 9, pp. 4590–4604, Sep. 2019.
- [7] L. Du, S. Shao, G. Yang, J. Ma, Q. Liang, and Y. Tang, "Capacity characterization for reconfigurable intelligent surfaces assisted multiple-antenna multicast," *IEEE Trans. Wireless Commun.*, vol. 20, no. 10, pp. 6940–6953, Oct. 2021.

- [8] G. Zhou, C. Pan, H. Ren, K. Wang, and A. Nallanathan, "Intelligent reflecting surface aided multigroup multicast MISO communication systems," *IEEE Trans. Signal Process.*, vol. 68, pp. 3236–3251, Apr. 2020.
- [9] F. Zhou, L. Feng, P. Yu, W. Li, X. Que, and L. Meng, "DRL-based low-latency content delivery for 6G massive vehicular IoT," *IEEE Internet Things J. (early access)*, Mar. 2021.
- [10] W. Hao, G. Sun, F. Zhou, D. Mi, J. Shi, P. Xiao, and V. C. Leung, "Energy-efficient hybrid precoding design for integrated multicast-unicast millimeter wave communications with SWIPT," *IEEE Trans. Veh. Technol.*, vol. 68, no. 11, pp. 10956–10968, Nov. 2019.
- [11] N. Chukhno, O. Chukhno, S. Pizzi, A. Molinaro, A. Iera, and G. Araniti, "Unsupervised learning for D2D-assisted multicast scheduling in mmwave networks," in *Proc. IEEE BMSB*, Chengdu, China, Oct. 2021, pp. 1–6.
- [12] Y. Mao, B. Clerckx, and V. O. K. Li, "Rate-splitting for multi-antenna non-orthogonal unicast and multicast transmission: Spectral and energy efficiency analysis," *IEEE Trans. Commun.*, vol. 67, no. 12, pp. 8754–8770, Sep. 2019.
- [13] I.-S. Cho and S. J. Baek, "Optimal multicast scheduling for millimeter wave networks leveraging directionality and reflections," in *Proc. IEEE INFOCOM*, Vancouver, Canada, May 2021, pp. 1–10.
- [14] G. Mendler and G. Heijenk, "On the potential of multicast in millimeter wave vehicular communications," in *Proc. IEEE VTC*, Helsinki, Finland, June 2021, pp. 1–7.
- [15] R. O. Afolabi, A. Dadlani, and K. Kim, "Multicast scheduling and resource allocation algorithms for OFDMA-based systems: A survey," *IEEE Commun. Surv. Tuts.*, vol. 15, no. 1, pp. 240–254, 1st Quart. 2013.
- [16] H. Won, H. Cai, D. Y. Eun, K. Guo, A. Netravali, I. Rhee, and K. Sabnani, "Multicast scheduling in cellular data networks," *IEEE Trans. Wireless Commun.*, vol. 8, no. 9, pp. 4540–4549, Oct. 2009.
- [17] H. Hao, C. Xu, M. Wang, L. Zhong, and D. O. Wu, "Stochastic cooperative multicast scheduling for cache-enabled and green 5G networks," in *Proc. IEEE ICC*, Shanghai, China, May 2019, pp. 1–6.
- [18] C. Huang, J. Zhang, H. V. Poor, and S. Cui, "Delay-energy tradeoff in multicast scheduling for green cellular systems," *IEEE J. Sel. Areas Commun.*, vol. 34, no. 5, pp. 1235–1249, May 2016.
- [19] B. Zhou, Y. Cui, and M. Tao, "Optimal dynamic multicast scheduling for cache-enabled content-centric wireless networks," *IEEE Trans. Commun.*, vol. 65, no. 7, pp. 2956–2970, Jul. 2017.
- [20] Z. Zhang, H. Chen, M. Hua, C. Li, Y. Huang, and L. Yang, "Double coded caching in ultra dense networks: Caching and multicast scheduling via deep reinforcement learning," *IEEE Trans. Commun.*, vol. 68, no. 2, pp. 1071–1086, Feb. 2020.
- [21] L. Zhong, C. Xu, J. Chen, W. Yan, S. Yang, and G.-M. Muntean, "Joint optimal multicast scheduling and caching for improved performance and energy saving in wireless heterogeneous networks," *IEEE Trans. Broadcast.*, vol. 67, no. 1, pp. 119–130, Mar. 2021.
- [22] D. P. Bertsekas, *Dynamic programming and optimal control: volume I*. Athena scientific Belmont, Belmont, MA, 2012.
- [23] R. Li, C. Huang, X. Qin, S. Jiang, N. Ma, and S. Cui, "Joint schedule of task- and data-oriented communications," in *Proc. IEEE GLOBECOM*, Rio de Janeiro, Brazil, Dec. 2022.
- [24] D. Tse and P. Viswanath, *Fundamentals of wireless communication*. Cambridge university press, Cambridge, 2005.
- [25] R. S. Sutton and A. G. Barto, *Reinforcement learning: An introduction*. MIT press, Cambridge, Massachusetts, 2018.
- [26] J. Schulman, F. Wolski, P. Dhariwal, A. Radford, and O. Klimov, "Proximal policy optimization algorithms," *arXiv preprint arXiv:1707.06347*, Jul. 2017.
- [27] G. Dulac-Arnold, R. Evans, H. van Hasselt, P. Sunehag, T. Lillicrap, J. Hunt, T. Mann, T. Weber, T. Degris, and B. Coppin, "Deep reinforcement learning in large discrete action spaces," *arXiv preprint arXiv:1512.07679*, Dec. 2015.
- [28] L. Huang, S. Bi, and Y.-J. A. Zhang, "Deep reinforcement learning for online computation offloading in wireless powered mobile-edge computing networks," *IEEE Trans. Mob. Comput.*, vol. 19, no. 11, pp. 2581–2593, Nov. 2020.

- [29] V. Mnih, K. Kavukcuoglu, D. Silver, A. A. Rusu, J. Veness, M. G. Bellemare, A. Graves, M. Riedmiller, A. K. Fidjeland, G. Ostrovski *et al.*, “Human-level control through deep reinforcement learning,” *Nature*, vol. 518, no. 7540, pp. 529–533, Feb. 2015.
- [30] C. Michele, G. Cornuejols, and G. Zambelli, *Integer programming*. Springer, Berlin, Germany, 2014.
- [31] H. Yu, S. Ruepp, and M. S. Berger, “Multi-level round-robin multicast scheduling with look-ahead mechanism,” in *Proc. IEEE ICC*, Kyoto, Japan, Jul. 2011.